YAN, Chengchu, et al. A seasonal cold storage system based on separate type heat pipe for sustainable building cooling. Renewable energy, 2016, 85: 880-889.

https://doi.org/10.1016/j.renene.2015.07.023 This is the Pre-Published Version.

A Seasonal Cold Storage System Based on Separate Type Heat Pipe for Sustainable Building Cooling

Chengchu Yan[a, b], Wenxing Shi[a]*, Xianting Li[a] and Shengwei Wang[b]

[a] Department of Building Science, Tsinghua University, Beijing, 100084, China

[b] Department of Building Services Engineering, The Hong Kong Polytechnic University, Hong Kong

* Corresponding author: Wenxing Shi, E-mail: wxshi@mail.tsinghua.edu.cn,

Phone: +86-10-62796114, Fax: +86-10-62773461

Abstract: Seasonal cold storage is a high-efficient and environmental-friendly technique that uses the stored natural cold energy in winter (e.g., snow, ice or cold ambient air) for free-cooling in summer. This paper presents a seasonal cold storage system that uses separate type heat pipes to charge the cold energy from ambient air in winter automatically, without consuming any energy. The charged cold energy is stored in the form of ice in an insulated tank and is extracted as chilled water for cooling supply in summer, which help to reduce the chiller running time and reduce the associated electricity consumption and greenhouse gas emission significantly A quasi-steady two-dimensional mathematical model of the system is developed for characterizing the dynamic performance of ice growth (i.e., cold charging). The model is validated using the field measurement data from an ice charging experiment conducted in Beijing. The impacts of various affecting factors, including the weather data and the key parameters of heat pipes, on the charging performance of the cold storage system are analyzed. The effectiveness and sustainability of the proposed system for cooling are demonstrated through a case study of a kindergarten building in Beijing.

Keywords: Seasonal cold storage; ice storage; heat pipe; renewable energy; sustainable cooling

1. Introduction

The worlds' cooling demand has increased significantly in the past decades due to the rapidly increased population, urbanization, comfort requirements and electronic equipment usage [1]. Conventional cooling is usually produced by electrically or thermally driven devices that consume a

large amount of fossil energy. By contrast, seasonal cold storage using the stored winter cold energy for cooling in summer is a less fossil energy-consuming alternative. This ancient technique date from two thousand years ago and it was widely used worldwide before the emergence of modern refrigerating technique. Seasonal cold storage is feasible in large parts of the world, particularly in cold regions such as northern Europe, Siberia, North America, Northeast and Northwest of China.

Due to the high energy efficiency and environmental benefits, modern applications of seasonal cold storage have attracted increasing attentions since the energy crisis from 1970s. Numerous seasonal cold storage techniques for cooling applications have been found. In Japan, about 100 projects have been implemented during the past 30 years and about 50-100 seasonal cold storage systems are found in China [2]. The first modem seasonal cold storage project for comfort air-conditioning was established by Princeton University in the late 1970s. The cold energy was stored in a big ice pond (with 10,000 m^3 capacity) and used to supply cooling for a 12,000 m^2 office building [3]. In Ottawa, Canada, the performance of using an abandoned rock quarry for the storage of 90,000 m^3 snow was studied [4]. Näslund investigated a district cooling system using stored snow in Sundsvall, Sweden. About 122,500 m^3 of snow, including the natural snow from streets and squares and the artificial snow made from snow guns or water spraying, was stored for providing the cooling energy that accounting for 43.6%~66.8% of the total cooling demand [5]. Hamada Y et al. investigated the effectiveness of a hybrid system for snow storage/melting and air conditioning on energy conservation and environmental protection through field measurements and numerical analyses [6]. Ground source heat pumps with earth heat exchangers or ground water offer a favorable cooling potential. In addition to the use of reversible ground source by heat pumps, the cold produced in wintertime can also be directly used for cooling in summertime, without running a refrigerant cycle [7].The performance data of 50 seasonal cold storage projects in four countries (Canada, Germany, The Netherlands and Sweden) were collected and analyzed by IEA (the International Energy Agency) in an annex entitled “Innovative and Cost-effective Seasonal Cold Storage Applications" [8]. Results shown that most seasonal cold storage projects have good cost-effectiveness with paybacks of five years or less.

The cooling sources of seasonal cold storage can be natural snow and ice, or artificial snow and ice produced from the cold ambient air, or the frozen soil and rocks in winter. Collecting natural snow or ice is the oldest and simplest way to obtain cold energy. It requires the least initial cost and consumes almost no auxiliary energy. The limitation is that collecting snow or ice exclusively is very labor-intensity and expensive [9]. In addition, the collected snow or ice usually contains many impurity substances that may corrode the chilled water pipes. In modern applications, the seasonal cold energy is usually charged from ambient cold air using snow guns, heat exchangers or heat pipes. Snow guns are the commonly used tools for producing snow. Two types of snow guns were used to produce snow for cooling supply in the Sundsvall Regional Hospital in Sweden. The pressurized water and air are sprayed separately and mixed in the air and the energy usage is 1~3 kWh per ton snow [10]. A seasonal cold storage project named “Icebox” was carried out in Canada [11]. The outdoor cold air was directly blown by fans into an indoor box to freeze the thinly sprayed water into ice layer by layer. The coefficient of performance (COP, i.e., the ratio between cooling energy to electricity consumption) in this Icebox project was about 90-100. The feasibility and performance of using the underground gravel mixed with ice for seasonal cold storage was studied by Illinois State University in the Gravel-Ice Storage Mass project [12]. The circulated antifreeze was firstly chilled-down by outdoor heat exchangers and then used to charge the cold energy into the mixture of gravel-ice by underground heat exchangers. Yang etc. proposed a similar seasonal soil cold storage system [13]. In winter, the system collects natural cold energy by outdoor air heat exchanger and stores it in soil by the U-tube using water-glycol mixture as refrigerant. Results show that the COP of the system ranges from 7.90 to 13.32. Although they are more energy efficient than conventional mechanical cooling, using aforementioned methods for cold charging still consume a certain amount of energy due to the usage of fans or pumps.

By contrast, seasonal cold storage using heat pipe might be a more attractive option in terms of energy efficiency since no additional energy is needed for cold charging. A heat pipe is a highly efficient heat-transfer device that can charge the cold energy from outdoor air into the cold storage medium automatically. Such technology has been successfully applied in frozen soil reinforcement and fruit and vegetable refrigeration projects. For example, a simple type of heat pipes, i.e.,

thermosyphons are commonly used as the seasonal cooling devices in permafrost areas for maintaining frozen conditions in the soil bases of buildings and structures [14]. In fact, the seasonal cold storage using heat pipes can be also used for comfort or process cooling in buildings. However, such investigations or studies are still very limited and only few studies can be found in the existing literature. For example, Singh etc. proposed a heat pipe based cold storage system for the thermal control system of a datacenter. Two types of cold energy storage, namely cold water storage and ice storage, can be realized in this system as daily based (night to day) or seasonal based (winter to summer) storage [15].

This paper therefore presents a novel seasonal cold storage system based on separate-type heat pipes for sustainable building cooling. It can store a large amount of cold energy without consuming any energy in winter and help to reduce the chiller running time in summer. Consequently, a massive amount of the electricity related cost and greenhouse gas emissions resulting from the electricity generation from non-renewable sources can be reduced. A quasi-steady two-dimensional mathematical model is developed for characterizing the dynamic process of ice growth (i.e., cold charging). The model is validated using the field measurement data from an ice charging experiment in Beijing. The impacts of key affecting factors, including weather data and heat pipes parameters, on the charging performance of the cold storage system are analyzed. A case study on the application of the proposed system for free cooling of a kindergarten building in Beijing is presented as well, which demonstrate the sustainability and effectiveness of the proposed system on energy conservation and environmental protection.

2. System Configuration and Operation Principle

The schematic of the proposed seasonal ice storage system is presented in Fig.1. The system consists of two parts or two subsystems, i.e., the cold charging subsystem and the cold discharging subsystem. In winter, the cold charging subsystem collects natural cold energy from the outdoor low-temperature air through separate type heat pipes to cools down the water in the underground tank until all water is frozen to be ice. In summer, the cold discharging subsystem extracts the stored cold energy by pumping chilled water through the discharging coilers, which are submerged into the

mixture of ice and melting water, to AHUs (air handling units) or FCUs (fan coil units) for air conditioning.

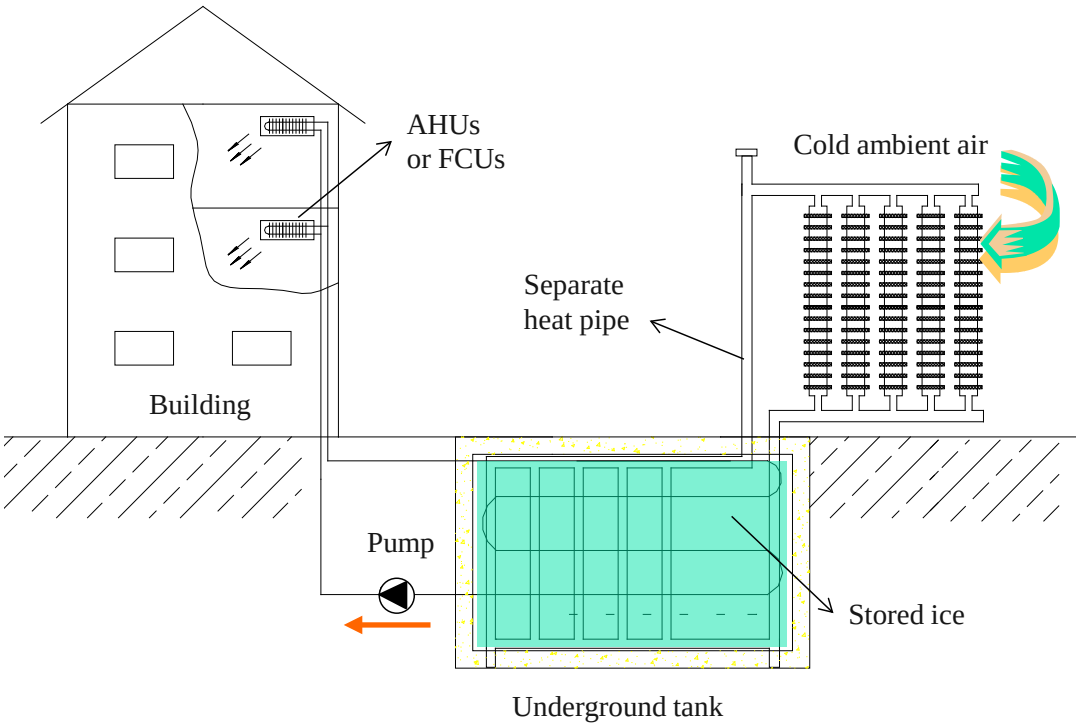

Fig.1 Schematic of the seasonal ice storage system using separate heat pipes

The working principle of separate heat pipes for cold charging can be illustrated using Fig.2. The cold charging device consists of a separate-type heat pipe and an ice storage tank. In a separate-type heat pipe, the evaporator segment and the condenser segment are separated in diffident locations. In this system, the evaporator is located in the ice storage tank (as heat source) and the condenser is located in the outdoor air (as heat sink). The altitude of the condenser should be higher than that of the evaporator so that the liquid working fluid (i.e., refrigerant) can return to evaporator by gravity. The heat pipe works as follows: In winter, when the outside air temperature is below the water temperature, the liquid refrigerant within the evaporator is heated into vapor. The vapor then travels along the vapor ascending pipe to condenser segment and condenses back into a liquid-releasing the latent heat to the outdoor air. The liquid then returns to the evaporator segment through the liquid descending pipe by gravity, and the cycle repeats. During this process, the water around the evaporator is frozen into ice gradually. Once the outdoor temperature is higher than the ice temperature, the heat pipe stops working automatically which ensures that only the one-way heat

transfer (i.e., heat release from the water tank to outdoor air) is allowed. The cold storage tank is typically located in underground and well-insulated to minimize the cold loss.

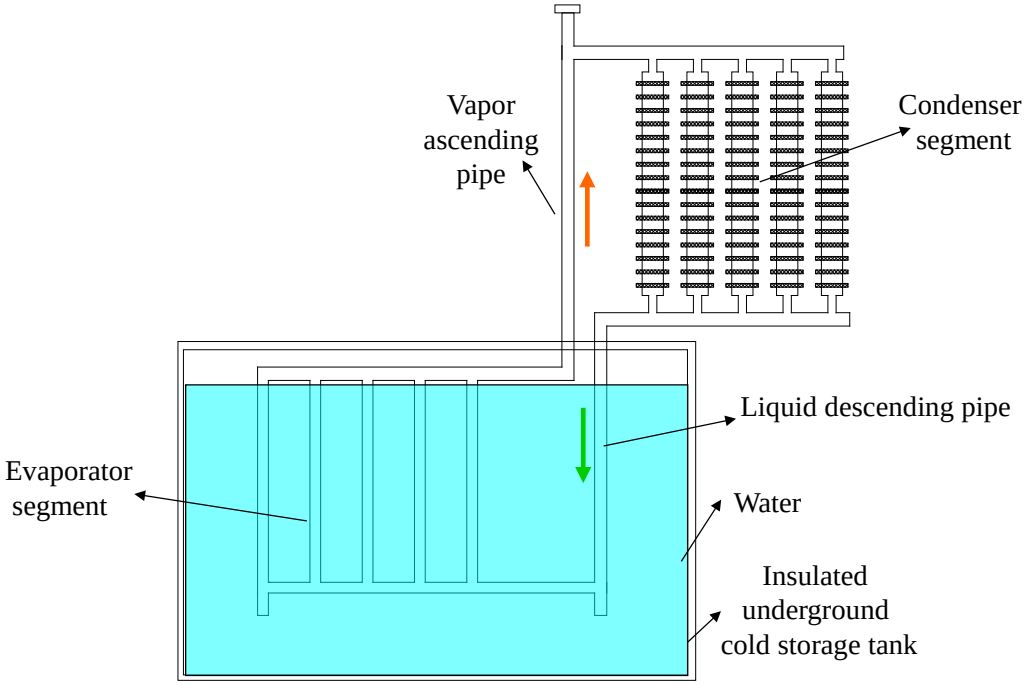

Fig.2 The configuration of separate heat pipes for cold charging

3. Mathematical Model for Cold Charging

In order to effectively analyze the dynamic cold charging performance of the seasonal cold storage system, a simplified physical configuration and a quasi-steady two-dimensional mathematical model are developed. The simplified configuration is used to describe the physical dimensions and key parameters of the cold charging device while the mathematical model is used to calculate the cold charging performance of the system by combining a series of heat transfer equations.

3.1 Simplifications on the physical configuration

A simplified physical configuration is used to highlight the dynamic process of the ice growth around the evaporator of the heat pipe. As shown in Fig.3, these parallel pipes in both the evaporator segment and the condenser segment are simplified as a single pipe in each segment. The evaporator pipe is a submerged plain tube for extracting the latent heat (i.e., Q_e) from water and making ice around the pipe. The condenser pipe is an externally finned tube exposing to the outside cold air for

heat rejection (i.e., Q_c) and refrigerant condensing. To prevent heat loss, the vapor ascending pipe and liquid descending pipe are insulated. More parameters of the heat pipe are as given in Table 1.

Table 1 Key parameters of the heat pipe for system modeling

	Evaporator	**Condenser**
Ambient temperature (°C)	Water temperature t_{water}	Outdoor air temperature t_{air}
Phase change temperatures (°C)	Evaporating temperature t_e	Condensing temperature t_c
Phase change heat transfer coefficient (W/ (m^2 • °C))	Evaporation coefficient h_e	Condensation coefficient h_c
Convection heat transfer coefficient (W/ (m^2 • °C))	h_{water} (convection between water and ice)	h_{air} (convection between air and pipe)
Pipe length (m)	L_e	L_c
Pipe diameter (mm)	$d_{i,e}$ (internal); $d_{o,e}$ (external)	$d_{i,c}$ (internal); $d_{o,c}$ (external)
Thermal conductivity (W/(m·K))	λ_e (evaporator pipe); λ_{ice} (ice layer)	λ_c (condenser pipe)

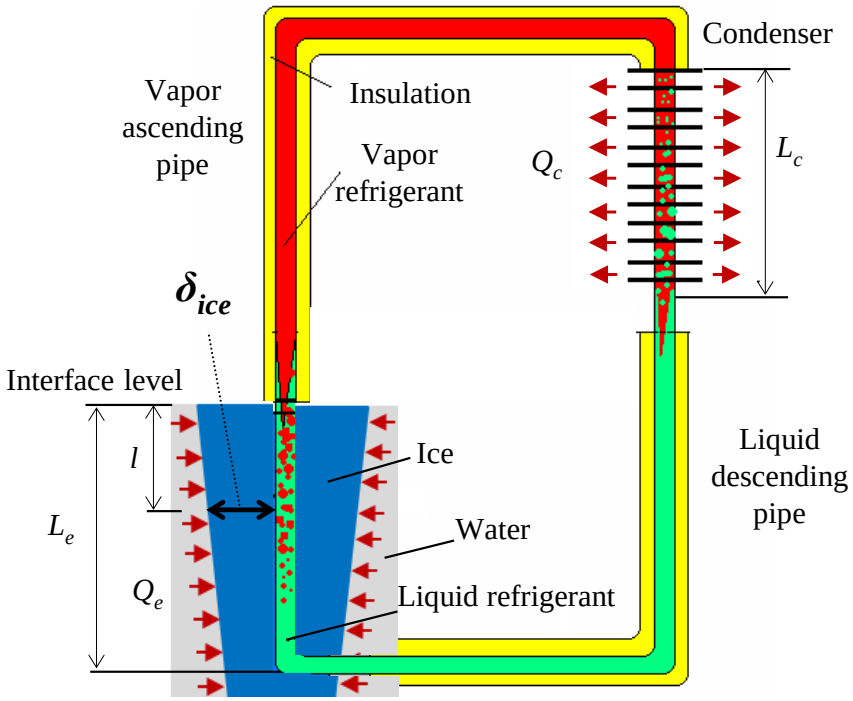

Fig.3 The simplified physical configuration of the cold charging device

It is worthy noticing that the ice thickness (i.e., δ_{ice}) around the evaporator pipe decreases significantly along the increase of the pipe depth (i.e., the vertical distance from the vapor-liquid interface level to a particular position, *l)*. This is the reason why the shape of the frozen ice looks like a cone rather than a cylinder in Fig.3. The ice growth rate is determined by the heat transfer rate between the water and the refrigerant through the evaporator: only when the saturated evaporating temperature of the liquid refrigerant is lower than the ice temperature (e.g., 0 °C), the boiling heat transfer can be started and ice is formed simultaneously. The larger distance from the interface level, the higher saturated evaporating temperature is caused by the higher static pressure.

3.2 *Quasi-steady two-dimensional model*

The cold charging process is a typical unsteady and non-uniform heat transfer process: 1) the temperature difference between the storage tank and outside varies all the time; 2) the thermal resistance of the heat pipe, particularly the resistance of the evaporator increases along with the increase of ice thickness around the pipe; and 3) the heat transfer rate varies significantly along the vertical direction of the evaporator. In this study, a quasi-static two-dimensional mathematical model is developed for calculating the ice thickness around the pipe in different time and different positions based on the following four assumptions:

1. The entire process of cold charging in winter is dynamic while heat transfer process within a short period of time $\Delta\tau$ (e.g., one hour) is considered to be steady-state.
2. The ice thicknesses (i.e., δ_{ice}) at different vertical positions (e.g., l) are different while the thickness within a short distance Δl is considered to be even.
3. Only the radial conduction is considered while the axial conduction is ignored within the ice.
4. If not specified otherwise, the heat loss of the vapor ascending pipe and liquid descending pipe, which are assumed to be insulated perfectly, can be ignored.

3.2.1 Condenser heat transfer

In condenser, three heat transfers occur in series: 1.) the condensation heat transfer between the refrigerant and the inside surface of the condenser pipe; 2.) the heat conduction through the condenser pipe; and 3.) the convection heat transfer between the outside surface of the condenser pipe and

outdoor cold air. By viewing the three heat transfers as a whole heat transfer through the cylinder, the heat released from the refrigerant to the outdoor air can be calculated in Eq. (1).

$$Q_c = K_c A_c \Delta t_c \tag{1}$$

where, A_c is the internal surface area of the condenser pipe, $A_c = \pi d_{i,c} L_c$;

Δt_c is the temperature difference of the refrigerant and the outdoor air, $\Delta t_c = t_c - t_{air}$;

K_c is the overall heat transfer coefficient in condenser when taking the internal surface area of the condenser pipe as reference, which can be calculated as following:

$$K_c = \left[\frac{1}{h_c} + \frac{d_{i,c}}{2\lambda_c} \ln \frac{d_{o,c}}{d_{i,c}} + \frac{1}{h_{air} \beta \eta_0} \frac{d_{i,c}}{d_{o,c}} \right]^{-1} \tag{2}$$

where, β and η_o are the external surface area coefficient and fin efficiency of the externally-finned pipes respectively.

3.2.2 Evaporator heat transfer

In evaporator, four different heat transfers occur in series: 1.) the boiling heat transfer between the refrigerant and the inside surface of the evaporator pipe; 2.) the heat conduction through the evaporator pipe; 3.) the heat conduction through the ice; and 4.) the convection heat transfer between the ice and the surrounding water. Considering that the heat transfer rates at different vertical positions are different, the heat transfer of the evaporator pipe should be divided into numerous sections (e.g., n even sections in this study). For a particular section with location of l and axial length of Δl, the extracted latent heat (ΔQ_e) from water to refrigerant can be calculated in Eq. (3).

$$\Delta Q_e(l) = K_e \Delta A_e \Delta t_e \tag{3}$$

where, ΔA_e is the internal surface area of the particular section l, $\Delta A_e = \pi d_{i,e} \Delta l$;

Δt_e is the temperature difference of tank water and refrigerant in section l, $\Delta t_e = t_{water} - t_e(l)$;

K_e is the overall heat transfer coefficient in section l when taking the internal surface area of the evaporator pipe as reference, which can be calculated as following:

$$K_e = \left[\frac{1}{h_e} + \frac{d_{i,e}}{2\lambda_e} \ln \frac{d_{o,e}}{d_{i,e}} + \frac{d_{i,e}}{2\lambda_{ice}} \ln \frac{d_{o,e} + 2\delta_{ice}(l)}{d_{o,e}} + \frac{1}{h_{water}} \frac{d_{i,e}}{d_{o,e} + 2\delta_{ice}(l)} \right]^{-1} \quad (4)$$

Accompanying with the heat transfer process in evaporator, fresh ice is formed around the section l. The mass of the freshly formed ice (Δm_{ice}) during $\Delta\tau$ can be calculated as following:

$$\Delta m_{ice} = \frac{\Delta Q_e(l) \cdot \Delta\tau}{1000 H_m} \quad (5)$$

where, H_m is the heat of fusion of water. During the ice formation process, the increased radial ice thickness ($\Delta\delta_{ice}$) in section l can be calculated in Eq. (6).

$$\Delta\delta_{ice}(l) = \frac{\Delta Q_e(l) \cdot \Delta\tau}{1000 \cdot H_m \cdot \rho_{ice} \cdot \pi \cdot [d_{o,e} + 2\delta_{ice}(l)] \cdot \Delta l} \quad (6)$$

The radial ice thickness around the evaporator pipe (δ_{ice}) increases gradually, which causes the overall heat transfer coefficient of evaporator (K_e) to be changed all the time. With the increased ice thickness, the total ice thickness can be updated in each time step, as shown in Eq. (7).

$$\delta_{ice}(\tau, l) = \delta_{ice}(\tau - \Delta\tau, l) + \Delta\delta_{ice}(\tau, l) \quad (7)$$

The heat transfer rate and ice thickness of other evaporator sections can also be calculated in the same way. The total heat transfer of the evaporator then can be obtained by summing up the heat transfer rate of all sections in the evaporator.

$$Q_e = \sum_1^n \Delta Q_e(l) \quad (8)$$

3.2.3 Phase change temperatures

The phase change temperature of water is constant, i.e., 0 °C. However, the phase change temperatures of the refrigerant are not constant and vary at different positions. Within the sealed volume of the heat pipe, a good corresponding relationship exists between the phase change temperature and the saturated pressure for a particular refrigerant. By assuming the absolute pressure of the refrigerant at the vapor-liquid interface as P_0, the pressure in the condenser pipe and the pressure in any position of the evaporator pipe then can be calculated, which can be used to determine the condensing and evaporating temperatures respectively.

For condenser, the pressure difference caused by the altitude difference as well as the pressure drop in the vapor ascending pipe can be ignored due to the low density of vapor and low velocity of vapor flow. As a result, the pressure in the condenser pipe can be considered as even and equals to p_0. The condensing temperature (t_c) then can be determined according to the correlation between saturated temperature and saturated pressure of the refrigerant.

$$t_c = f(P_0) \tag{9}$$

By contrast, the situation in evaporator is different. In the evaporator pipe, the static pressure difference caused by the altitude difference of the liquid refrigerant is very considerable. The absolute pressure of a particular location l can be calculated as following:

$$P(l) = P_0 + \rho_l g l \tag{10}$$

where, ρ_l is the density of liquid refrigerant, l is vertical distance below the liquid-vapor interface. The saturated evaporating temperature at this position then can be determined accordingly.

$$t_e(l) = f[P(l)] \tag{11}$$

3.2.4 Numerical algorithm

In order to solve above complicated and coupled heat transfer equations, a numerical algorithm is proposed for calculating the ice thickness and heat transfer rates. The principle of the algorithm is the energy balance within the heat pipe. In a certain period of time $\Delta\tau$ (e.g., one hour), the rejected heat by the condenser (Q_c) should be equal to the absorbed heat by the evaporator (Q_e). As analyzed above, the assumed value of P_0 (i.e., the pressure in the vapor-liquid interface) determines the condensing and evaporating temperatures of the heat pipe, and then affects the heat transfer of condenser and evaporator. Whether the assumed value is correct or not can be indicated by the heat balance residual, which is defined as following:

$$\mu = \frac{\left| Q_c - Q_e \right|}{0.5 \times (Q_c + Q_e)} \tag{12}$$

where, μ is the relative difference of heat between the condenser and evaporator. Different μ is resulted by different assumed P_0. When the value of μ is less than a predefined threshold μ_0, the

energy balance is considered to be achieved. In other words, the correct value of p_0 is identified only when the heat balance residual is small enough.

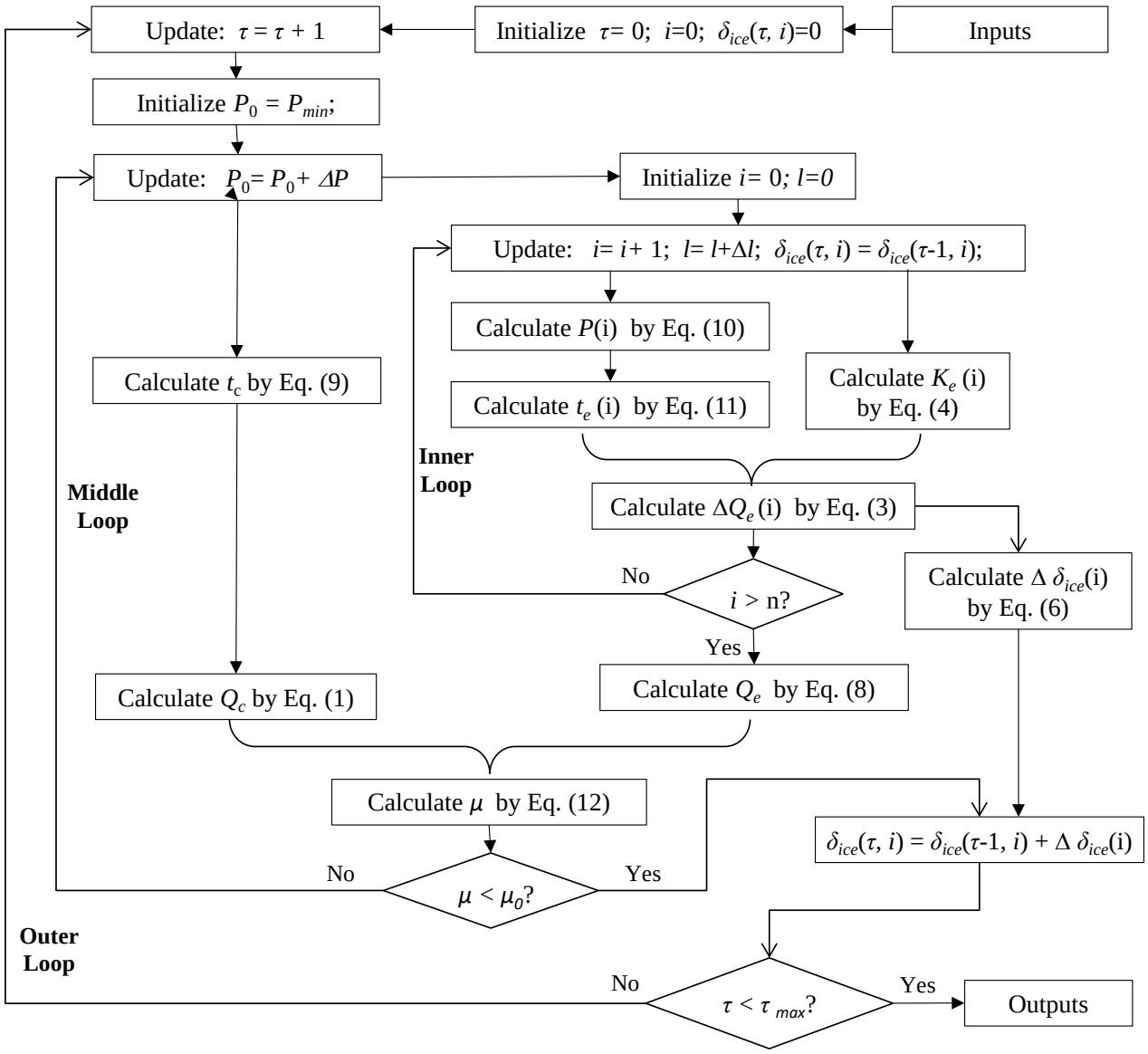

Fig.4 Flow chart of the numerical algorithm for cold charging

The flow chart of the numerical algorithm for cold charging is presented in Fig.4. The algorithm consists of three nested loops. The first loop (i.e., the outer loop) is for charging time traversing, in which the radial ice thickness (δ_{ice}) is calculated hour by hour. The second loop (i.e., the middle loop) is for refrigerant pressure traversing, in which the correct pressures of the liquid-vapor interface in each time step are identified based on the heat balance between the condenser and evaporator. The

third loop (i.e., the inner loop) is for the evaporator section traversing, in which the ice growth rate of each section of the evaporator is calculated from top to bottom.

The incremental steps in these loops are determined based on the overall consideration of both the computation time and the calculation accuracy. In the outer loop, the time step is determined as one hour. This is mainly because the weather data (e.g., the outside temperature and wind velocity) are updated once an hour. In the middle loop, ΔP =0.001(P_{max}-P_{min}). P_{max} and P_{min} are the saturated pressure of the refrigerant corresponding to the ice temperature (0°C) and the outdoor air temperature respectively. The predefined threshold μ_0 is set as 0.001. In the inner loop, $\Delta l = L_e/n$, and n=100. More tiny incremental steps can further refine the calculation accuracy while the longer computation time is required.

4. Experimental Validation of the Model

a. Experimental heat pipe b. Charged ice in the storage tank

Fig.5 Experimental cold charging system

The developed cold charging model was validated in a five-day experiment (from 12th to 16th in January) in Beijing. The experimental heat pipe device is formed by two identical parallel connected heat pipes as shown in Fig.5. After the air in the heat pipe is removed by a vacuum pump, refrigerant R-22 is full-filled into the evaporator pipe as the working fluid and then sealed. The heat pipes are made from stainless steel tubes and coated with a thin layer of red anti-rust paint. Each heat pipe has

three evaporator pipes with the length of 0.6m and the diameter of 32mm. The outdoor air temperature and wind speed during the experimental period were recorded by data logs continuously (see Fig.6). The ice thickness of three evaporator pipes (marked as 1, 2 and 3) in three positions (i.e., Top with l=0m, Middle with l=0.3m, and Bottom with l=0.6m) were measured manually once a day.

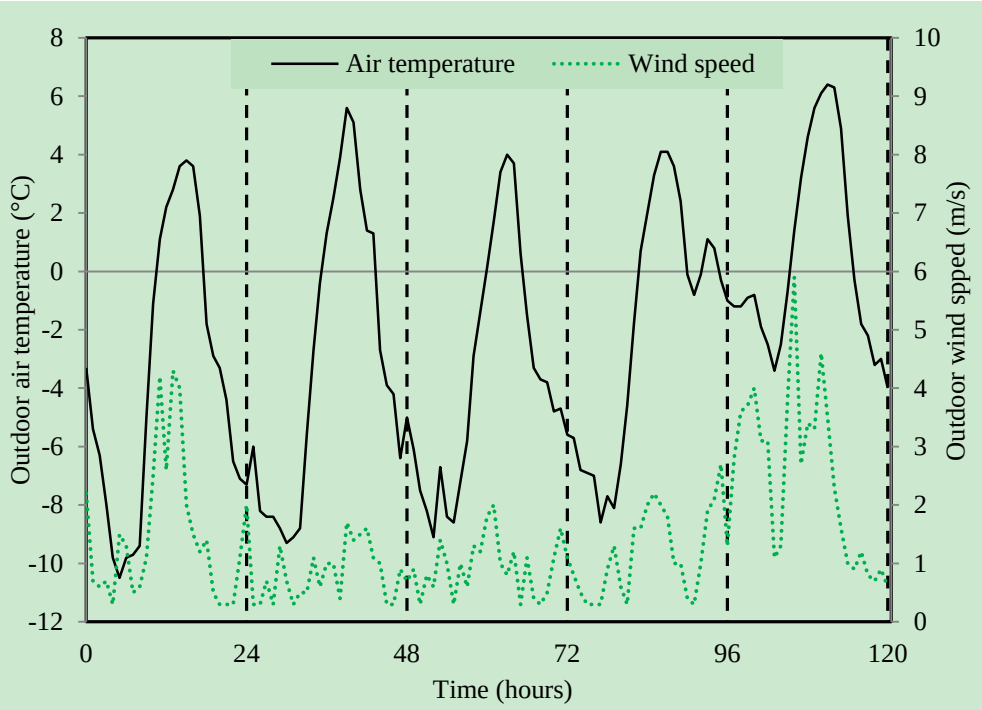

Fig.6 Outdoor air temperature and wind speed during the experiment

The cold charging performances calculated from the developed model are compared with that from the measured data in the experiment. It is worth noting that the vapor ascending pipe and liquid descending pipe of the experimental system are not insulated due to their limited lengths and complicated connections, which are different from the conditions described in Fig 3. In order to simulate the performance of the system under the same conditions of the experiment, the calculation model is slightly adjusted by viewing the surface area of all exposed parts of the system as the condenser area when calculating the heat rejection of the condenser sector. The ice thickness (δ_{ice}) of three evaporator pipes in the middle position (l=0.3m) are presented in Fig.7. It can be observed that the ice thickness differences among these three pipes are very limited and all these experimental data agree well with the calculated data using the developed model. It can also be observed that the ice growth rate is strongly dependent on the outdoor air temperature. At the beginning of the experiment

(the first day), the heat pipe first cooled down the water from the room temperature to freezing point and then frozen the water into ice. The ice thickness increased rapidly in nighttime when the outdoor temperature was lower than 0°C. The increase was stopped in daytimes as the heat pipe stopped working when the outdoor temperature rose above 0°C.

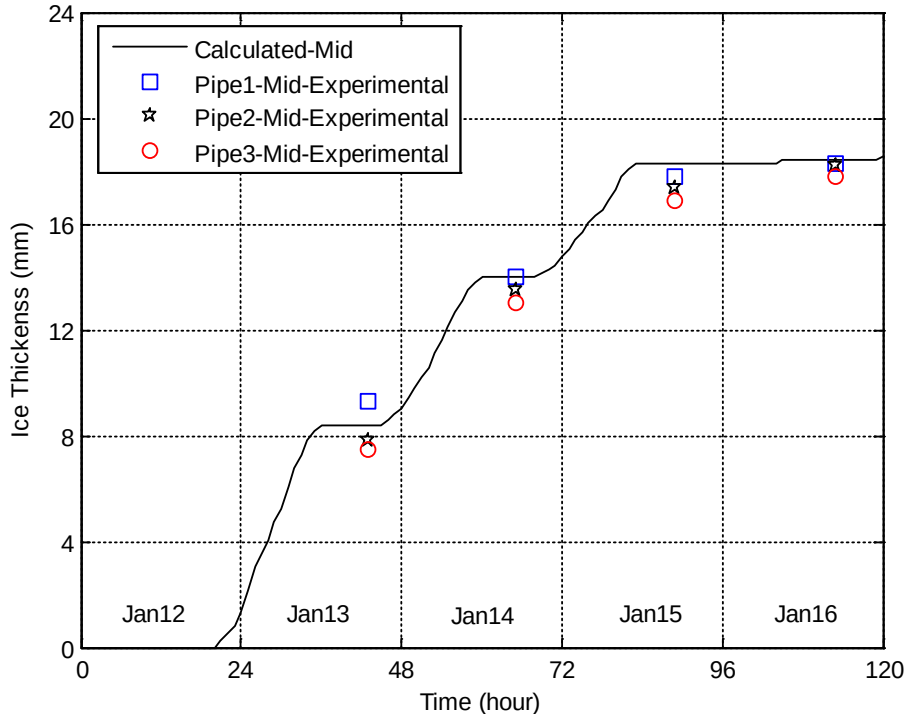

Fig.7 Ice thickness of three evaporator pipes in the middle position (l=0.3m)

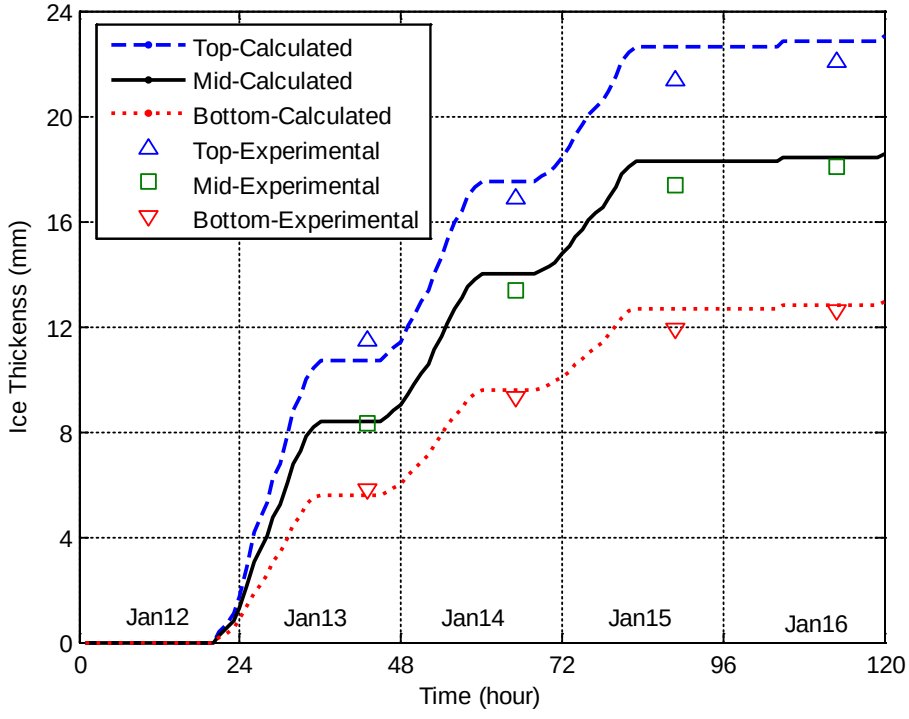

Fig.8 Average ice thickness of three evaporator pipes in different positions

The average ice thicknesses of three evaporator pipes in different positions are presented in Fig. 8. The measured data agreed well with the calculated data in most points. The ice growth rates in different positions were different significantly. The ice thicknesses at the top were almost as twice as that in the bottom. The ice thickness difference between the top position and bottom position would be more evident if the length of evaporator pipe is larger.

5. Charging Performance Analysis

The key factors affecting the charging performance including the weather data and heat pipe parameters are analyzed using the developed model. If not specified otherwise, the data and parameters used for the analysis are as follows: The external diameter (Φ_o) of the evaporator and condenser pipe is 32 mm. The total length of the evaporator pipe (L_e) is 1m and the concerned ice thickness is in the middle of the pipe (l=0.5). The surface area of the condenser and evaporator are the same. The condenser pipe is non-finned (i.e. $\beta\eta_o$=1). The outdoor wind speed is 1m/s. The outdoor air temperature data are the TMY (Typical Meteorological Year) data from the database of DeST [16].

5.1. The impact of weather data

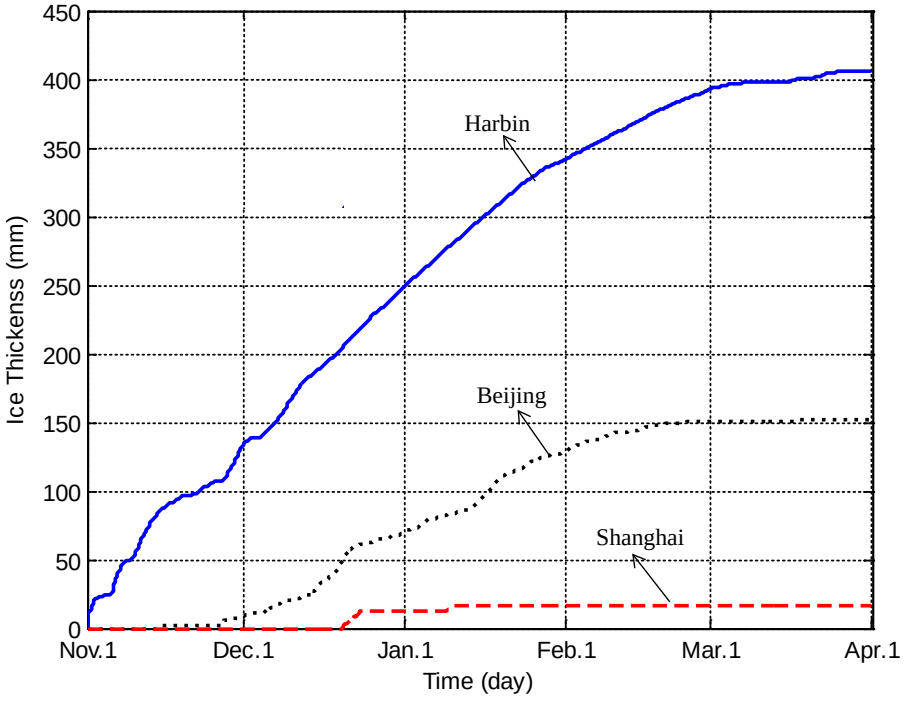

Fig.9 Ice thickness of three cities located in different climates

The outdoor temperature is the most important factor in determining the cold charging performance. The impact of outdoor air temperature on the ice thickness is presented in Fig.9. The freezing degree-hours (FDH) is an indicator that can indicate both the duration and magnitude of below-freezing temperatures during a specified period. The cumulative values of FDH for a winter (e.g., from Nov.1 to Apr.1 in this study) can tell how cold it has been for how long. The cold charging performances of three cities in China (i.e., Harbin, Beijing and Shanghai, which represent the severe cold, cold and mild climates respectively) are compared. The freezing degree-hours of Harbin, Beijing and Shanghai are 42776 (°C·H), 6821 (°C·H) and 265(°C·H) respectively. It can be observed that the ice thicknesses are greatly different in these three cities. The thickness by the end of cold charge can be larger than 400 mm in Harbin while the value is less than 20 mm in Shanghai.

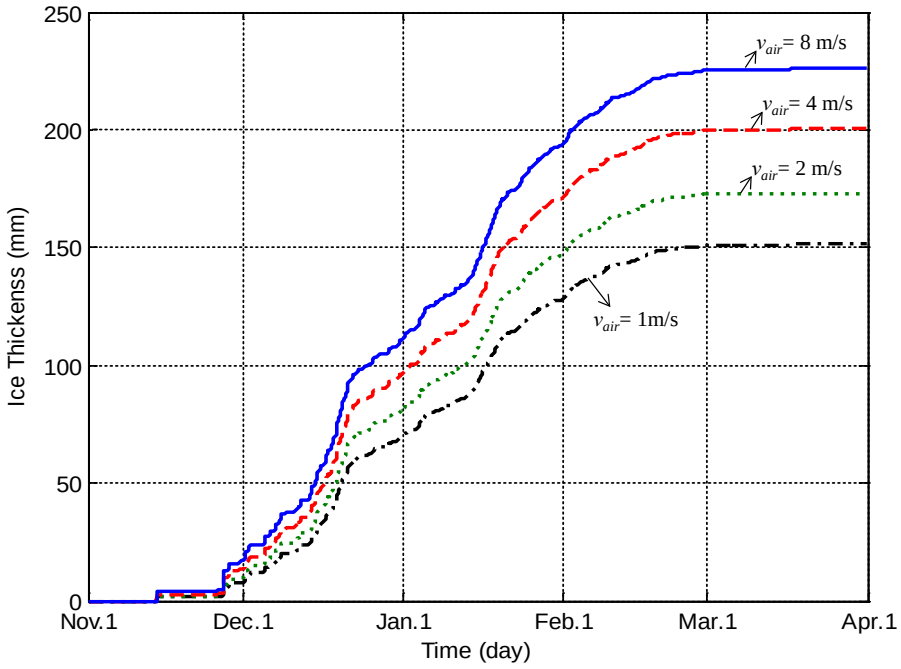

Fig. 10 Ice thickness with different wind velocity in Beijing

The wind speed (v_{air}) also plays an important role in determining the cold charging performance. Different wind speed results different heat transfer coefficient of wind that is the controlling factor in the heat transfer of condenser. The ice charging curves under different wind speed are presented in Fig.10. The results are expectable: larger wind speed brings better charging performance. Some

useful measures might help increase the outdoor wind speed: placing the condenser at higher place without blocking, using the air deflector to induce a higher wind's velocity over the condenser, etc.

5.2. The impact of condenser area

Enlarging the effective condenser area by using the externally finned tube has the similar effect as increasing the outdoor wind speed. As shown in Fig.11, the ice thickness is increased significantly when the effective condenser area (indicating by the value of $\beta\eta_o$) is enlarged. The larger condenser area means consuming more metal material. As a result, a cost-effectiveness analysis is needed when considering using this method for charging performance enhancement.

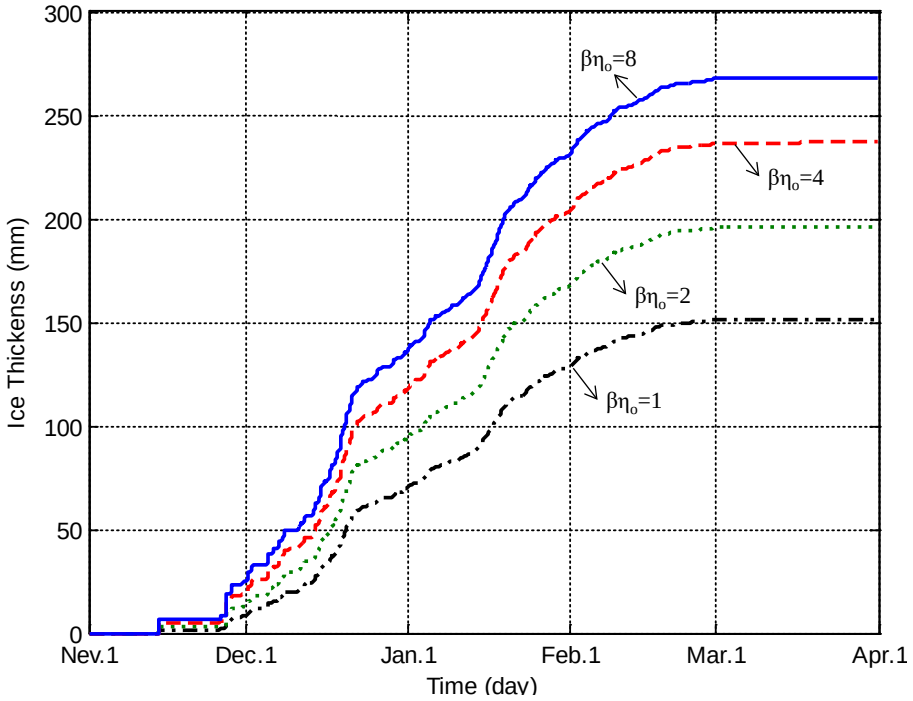

Fig.11 Ice thickness with different effective condenser area in Beijing

5.3. The impact of evaporator size

The diameter and length of the evaporator pipe also have impact on the charging performance. Fig.12 presents the cold charging curves of the evaporator with different diameters. It can be observed that the larger diameter has larger ice thickness. However, the increase rate of the charged ice due to the larger diameter is less than the increase rate of need metal materials and refrigerant associated. For example, when the diameter (Φ_o) is increased from 15mm to120mm, the final ice thickness is

increased less than twice, which means the charged cold is increased less than four times. But the mass of the metal and refrigerant is increased much more than four times. As a result, using the small diameter pipe is more cost-effective than using the larger one.

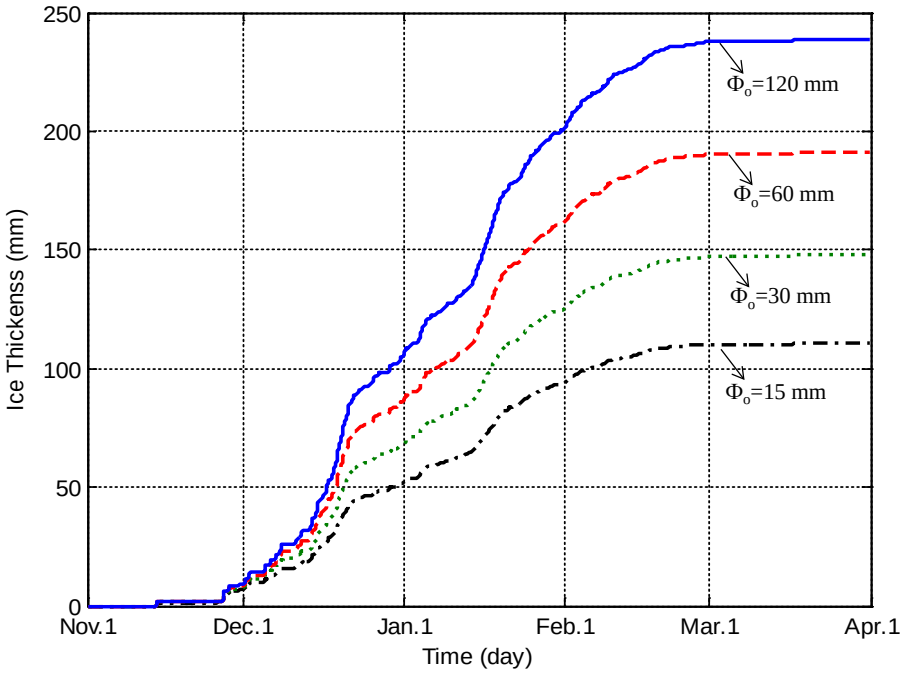

Fig.12 Ice thickness with different evaporator diameter (Φ_o) in Beijing

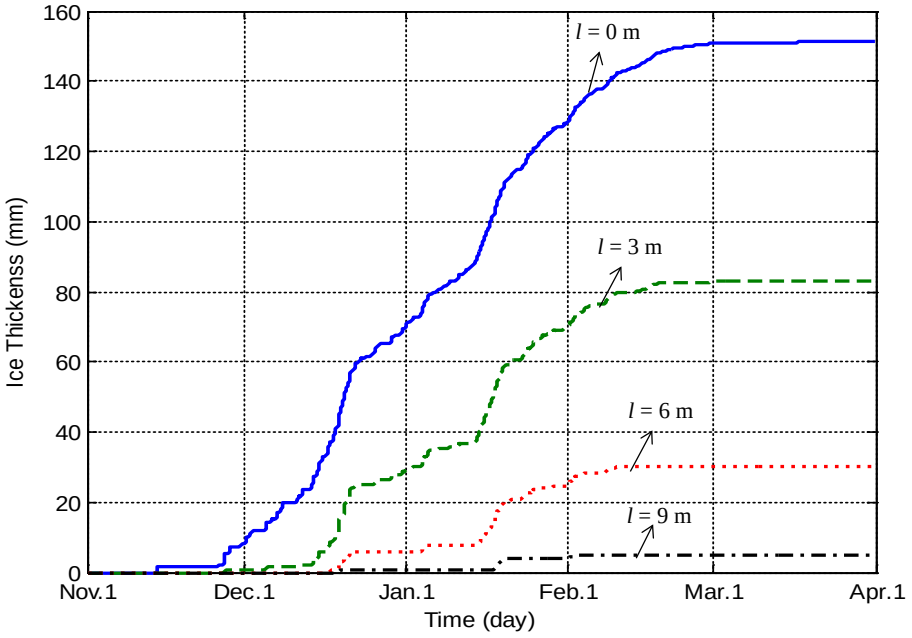

Fig.13 Ice thickness with different evaporator length (l) in Beijing

Fig.13 shows the impact of the evaporator length on the ice charging performance. The ice thickness in the top (l≈0m) of the evaporator can reach 150mm and it decreases rapidly with the increase of pipe

length. When the evaporator tube length is 9m, the δ_{ice} in the bottom is less than 10mm. For refrigerant R22, the static pressure increase caused by the gravity force of 9m liquid can make the saturated evaporating temperature in this position to be 9°C higher than that in liquid-vapor interface. In order to avoid a large difference of ice thickness in the top and bottom, the shorter pipe and lower-density refrigerant are preferred.

6. Application in a Real Building

6.1. Building description

The proposed seasonal cold storage system is applied in a kindergarten building in Beijing. The total gross area of this building is about 2000 m^2, which aims to be a low-energy sustainable building through using various renewable energy including solar energy, under-ground thermal energy and natural cold energy in winter. The cold energy utilization is realized by using the proposed seasonal cold storage system for free cooling. In this building, the cooling period is from April to November. The hourly cooling load is presented in Fig.14 and the total cooling demand of the cooling season is about 83.1MWh.

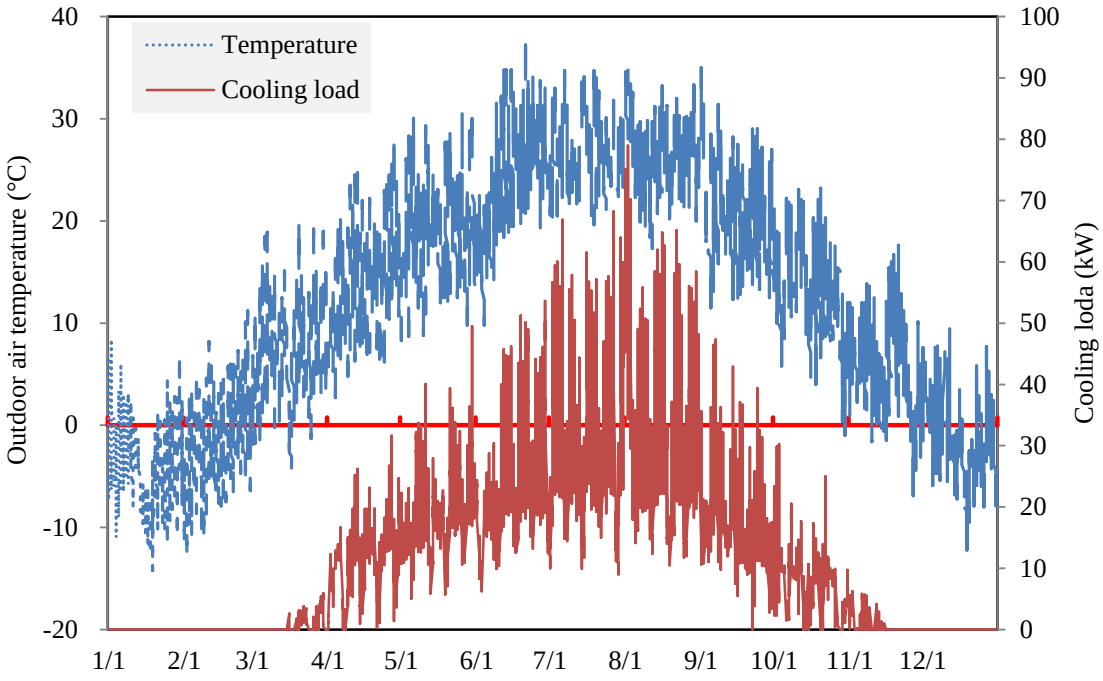

Fig.14 Outdoor air temperature and cooling load of the building

6.2. Implementation and performance

A compound cooling system combing a seasonal ice storage system and a traditional electrical chiller is used in the building and a large part of the total cooling demand is supplied by the seasonal cold storage system. The main components of the implemented seasonal cold storage system are shown in Fig.15. The key parameters of the heat pipe and the performances of the system, which significantly determines the energy performance of the building and the cost-effectiveness of the system, are presented in Table 2. The most important parameter for the cold storage system is the storage capacity. The larger capacity designed, the less energy needed for cooling while the larger initial cost involved. In this case study, about one third of the total cooling demand should be provided by the seasonal cold storage system to help achieve the goal of low-energy cooling in this sustainable building. The volume of the storage tank is then determined by the storage capacity and the cold storage density (about 70 kWh/m^3) of ice. According to the analysis results in section 5 and some practical constrains (e.g., the strength requirement and available space for tank layout), the pipes with small diameter (Φo =25mm) and short length (3m) are selected. The outdoor condenser consists of a cluster of externally-finned pipes in parallel and hundreds of evaporator pipes are immersed in an insulted underground water tank. Based on a simplified cost-effectiveness analysis, the surface area ratio between the condenser and the evaporator is selected to be two ($\beta\eta_o$=2). Concerning the selection of refrigerant, the safety issue is considered as the important factor in a kindergarten building. This is the main reason why R22 rather than ammonia is selected in this project even though ammonia is a better refrigerant than R22 in terms of the price, the cold charging performance and environmental performance.

Table 2 Key parameters of the implemented seasonal cold storage system

Heat pipe	*Material and thickness:* Stainless steel pipe Φo =25mm	*Surface area:* Evaporator 375 m^2 Condenser 750 m^2	*Charged Refrigerant:* R22
Storage tank	*Volume:* 450m^3	*Tank depth:* 3.5m	*Storage capacity:* 31,500 kWh

Insulation	*Material and thickness:* XPS(Extruded polystyrene) 100mm	*Overall heat-transfer coefficient*: 0.3W/m^2·℃	*Seasonable cold loss rate:* <10%

Fig.15 Implementation of the seasonal cold storage system

This seasonal cold storage system has been put into operation with satisfied performance since 2008. The outdoor air temperature in the winter of Beijing is below 0 °C in most of the time (see Fig.14), which enables a long period of time for cold charging. By the end of each March, the tank is almost fully charged with ice. The charged cold energy is about 31,500 kWh per year, which can provide free cooling in the building by the end of June or early July. Considering that the cold loss rate during the storage and usage periods is about 10%, the system can provide effective cold energy about 28,350 kWh for cooling, accounting for 34.1% of the total cooling demand. The simple payback time of the system is estimated between 8~10 years in this case study. This time is expected to be reduced significantly, if the system is located in colder regions (e.g., Harbin).

7. Conclusion

A seasonal cold storage system that uses the natural cold energy in winter is developed for sustainable building cooling in this paper. The cold energy is charged into a tank in the form of ice by a separate type heat pipes automatically and provided as free cooling in summer. A mathematic model is developed and validated for analyzing the cold charging performance. A case study on the application of the seasonal cold storage system in a real building is presented as well. The concluding remarks from this study are drawn as follows.

(1) Seasonal cold storage is an energy-efficient and environmental-friendly technique for sustainable free cooling in buildings located in appropriate climates. A separate-type heat pipe can be used as an effective and energy-free device for cold charging.

(2) The cold charging process of the proposed seasonal cold storage system is a complicated unsteady and non-uniform heat transfer process, which can be molded by the developed quasi-steady two-dimensional model. The developed model was well validated by a cold charging experiment.

(3) The outdoor temperature is the most important factor in determining the charging performance. The system performs well in cold or severe cold regions in china. Enlarging the condenser area and increasing the outdoor wind speed can enhance the charging performance significantly. The ice thickness around the evaporator pipe decreases rapidly with the increase of pipe length. Selecting the shorter evaporator pipe and lower-density refrigerant can help reduce the ice thickness difference along the pipe and enhance the charging performance of the system.

(4) The proposed system is implemented and operated successfully in a real building in Beijing. The operation results show that a system with the storage volume of 450 m^3 can provide about 1/3 of the total cooling demand of a building with total gross area of 2000 m^2. The payback time of the system is about 8~10 years in this case study.

Acknowledgements

The research presented in this paper is financially supported by a grant (5267/13E) of the Research Grant Council (RGC) of the Hong Kong SAR and a grant (No. 51176084) of the National Natural Science Foundation of China, which are greatly appreciated.

References

[1]. Paksoy H Ö. General State-of-The-Art Report, Subtask 1. Annex 14, Cooling in all climates with thermal energy storage. July 2003. International Energy Agency (IEA), Energy Conservation through Energy Storage (ECES).

[2]. Kaneko Y, Kobiyama M, Nagaoke H, Sato T (2000). Air-conditioning System for Apartment Residences by Using Water made from Snow. Paper for ISCORD 2000. Conference in Hobart, Australia.

[3]. Kirkpatrick D L, Masoero M, Rabl A, et al. The ice pond-production and seasonal storage of ice for cooling. Solar energy, 1985, 35(5): 435-445.

[4]. Morofsky E (1981). Project Snowbowl. Public Works of Canada (PWC) Contract EN 280-0-3650.

[5]. Näslund M (2000). District cooling in Sundsvall based on sea water and stroed snow. Master thesis 2000:132 CIV, Luleå university of technology, Department of Environmental Engineering, Division of Water Resources Engineering, Sweden.

[6]. Hamada, Yasuhiro, Makoto Nakamura, and Hideki Kubota. Field measurements and analyses for a hybrid system for snow storage/melting and air conditioning by using renewable energy. Applied energy 84.2 (2007): 117-134.

[7]. Sanner B. Ground coupled heat pumps with seasonal cold storage. Proceedings of the International Energy Agency Heat Pump Conference, Published by Elsevier Science Publishers. 1993: 301.

[8]. Morofsky, E. (1997). Seasonal cold storage building and process applications: a standard design option. In MEGASTOCK'97 Proc. of the 7th International Conference on Thermal Energy Storage, Sapporo, Japan (pp. 1009-1014).

[9]. Johansson P (1999). Seasonal cold storage in rock caverns. Master thesis 1999:184 CIV, Luleå university of technology, Department of Environmental Engineering, Division of Water Resources Engineering, Sweden.

[10].Kjell Skogsberg. The Sundsvall Regional Hospital snow cooling plant—results from the first year of operation. Cold regions science and technology. 2002, 34:135-142.

[11].Jacob Klassen. Project Icebox-And Annual Energy Storage System. ASHRAE Transactions. 1981, 87(1): 1456-1460.

[12].C.E.Francis, R.T.Tamblyn. Annual Cycle Ice Production and Storage ASHRAE Transactions. 1987, 93(Pt.1):1760-1765.

[13].Yang, T., Zhang, X., Zhou, B., & Zheng, M. (2013). Simulation and experimental validation of soil cool storage with seasonal natural energy. Energy and Buildings, 63, 98-107.

[14].Popov A P, Vaaz S L, Usachev A A. Review of the current conditions for the application of heat pipes (thermosyphons) to stabilize the temperature of soil bases under facilities in the far North. Heat Pipe Science and Technology, An International Journal, 2010, 1(1).

[15].Singh, R., Mochizuki, M., Mashiko, K., & Nguyen, T. Heat pipe based cold energy storage systems for datacenter energy conservation. Energy 36.5 (2011): 2802-2811.

[16].Crawley D B, Hand J W, Kummert M, et al. Contrasting the capabilities of building energy performance simulation programs. Building and environment, 2008, 43(4): 661-673.